JOURNAL OF CATALYSIS 155, 353–365 (1995)

Activation Studies with a Precipitated Iron Catalyst for Fischer–Tropsch Synthesis

I. Characterization Studies

Dragomir B. Bukur,*[,1] Kiyomi Okabe,*[,2] Michael P. Rosynek,† Chiuping Li,† Dingjun Wang,† K. R. P. M. Rao,‡ and G. P. Huffman‡

*Department of Chemical Engineering, Kinetics, Catalysis, and Chemical Reaction Engineering Laboratory, Texas A & M University, College Station, Texas 77843-3122; †Department of Chemistry, Texas A & M University, College Station, Texas 77843-3255; and ‡The Consortium for Fossil Fuel Liquefaction Science, University of Kentucky, Lexington, Kentucky 40506-0107

Received September 14, 1994; accepted May 18, 1995

A commercial promoted precipitated iron catalyst (100 Fe/5 Cu/4.2 K/25 SiO_2 by weight) was characterized after different pretreatment conditions and after Fischer–Tropsch (FT) synthesis in a fixed bed reactor. The BET-N_2 surface area and pore volume of the catalyst decreased after pretreatments in hydrogen, carbon monoxide, or syngas. Isothermal and temperature-programmed reduction profiles indicate that iron reduction occurs in two steps: facile reduction of Fe_2O_3 to Fe_3O_4, followed by slow reduction of Fe_3O_4 to either metallic iron (H_2 reduction) or an iron carbide (CO pretreatment). Calcined catalyst is in the form of poorly crystalline α-Fe_2O_3, which is partially converted to either magnetite (Fe_3O_4) or a mixture of α-Fe and Fe_3O_4 after H_2 reductions. During FT synthesis the α-Fe and a portion of iron oxides are carburized to a pseudo-hexagonal ε'-$Fe_{2.2}C$. After CO or syngas pretreatments, the hematite is partly converted to a monoclinic χ-Fe_5C_2 carbide. During FT synthesis this carbide is partially converted to magnetite. The degree of surface iron reduction, determined by X-ray photoelectron spectroscopy, was greater after the CO pretreatment at 300°C for 4 h than that obtained after the H_2 reduction under the same conditions. However, in both cases a fraction of the surface iron remained in the form of unreduced Fe^{2+}/Fe^{3+} species. Also, the surface carbon deposits were formed during the CO pretreatment. © 1995 Academic Press, Inc.

INTRODUCTION

There is a large number of studies in the literature dealing with the issue of the role of iron phases in Fischer–Tropsch (FT) synthesis (1–12). Typically, these studies were conducted with model catalyst systems (e.g., iron supported on alumina, silica, and other supports), at atmospheric pressure, with H_2-rich syngas mixtures (H_2/CO = 3 or higher), over short periods of time (several hours on stream), and at low (differential) conversions. In the majority of these studies a catalyst precursor was completely reduced with H_2 prior to exposure to synthesis gas, and conversion of metallic iron to iron carbide phases was followed as a function of time (usually by Mössbauer effect spectroscopy, MES), while changes in gas phase composition were monitored with an on-line GC or a mass spectrometer. In some of these studies precarbided (1, 2) and oxidized (2–4) catalysts were used. In studies where the catalyst precursor was completely reduced prior to FT synthesis it was found that rate of FT synthesis (FTS) as a function of time-on-stream passes through a maximum. Several models have been proposed to explain this type of behavior, and the two which are most frequently cited are the carbide model (5–7) and the competition model (8). In the carbide model iron is not considered to be active for the FT synthesis, but the surface carbides with its underlying iron carbide bulk structure are, whereas in the competition model iron atoms at the surface are considered as the active sites. In the latter model both bulk carbidation and FT synthesis (hydrocarbon formation) have a common surface carbidic precursor. In addition to these two postulates concerning the nature of the active phase, Teichner and co-workers proposed that magnetite (Fe_3O_4) is the active phase in FT synthesis (4, 9). Validity of the latter proposal was questioned (10), but some evidence in its support has also been presented (2, 11, 12).

Due to its technological importance, the effect of activation parameters on catalyst performance during FTS was examined in several studies (13–18). Results from these

[1] To whom correspondence should be addressed. FAX: (409) 845-6446; E-mail: dbb7627@chennov1.tamu.edu.

[2] Present address: National Chemical Laboratory for Industry, Tsukuba, Ibaraki 305, JAPAN.

0021-9517/95 $12.00

studies show that activation parameters may have a significant effect on subsequent catalyst FT activity, selectivity, and stability. However, in the absence of simultaneous comprehensive catalyst characterization studies, the underlying reasons for differences in catalytic behaviors during FT synthesis are still not well understood.

Recently, two characterization studies were conducted with a commercial precipitated iron catalyst prepared by Ruhrchemie (19–21). This catalyst was used initially in commercial fixed bed reactors at SASOL in South Africa (22). In a study by Lox *et al.* (19) the catalyst was characterized by a variety of methods: BET surface area and pore size distribution, X-ray difraction (XRD), MES, temperature-programmed reduction (TPR), and X-ray photoelectron spectroscopy (XPS), after reduction with hydrogen at 220°C and after FT synthesis. The Ruhrchemie catalyst and a catalyst with nominal composition 100 Fe/3 Cu/0.2 K were characterized at Sandia National Laboratory (20, 21) by Auger electron spectroscopy (AES), BET, and transmission electron microscopy, after activations with hydrogen (at 220 to 280°C) and carbon monoxide (at 280°C). Relatively small variations in syngas conversions (55–64%) obtained in tests with the Ruhrchemie catalyst conducted in our Laboratory (23), utilizing three different pretreatment procedures, were consistent with the observed similarities in its surface compositions in their study utilizing AES (20, 21).

In the present study we investigated effects of five activation (pretreatment) procedures on textural properties (BET), reducibility of iron (TPR, isothermal reduction, and XPS), and the nature of initial bulk iron phases (XRD, MES) in the Ruhrchemie catalyst. Also, the pretreated catalysts were exposed to a synthesis gas under reaction conditions representative of industrial practice to study effects of pretreatment conditions on the catalyst activity and selectivity. Catalyst samples withdrawn from a fixed bed reactor at the conclusion of each of the six tests (100–630 h in duration) were characterizd by XRD and MES to determine bulk iron phases in the working catalyst. This study is more comprehensive than the one conducted at Sandia National Laboratory (20, 21) in several respects: (1) a wider range of pretreatment conditions and catalyst characterization techniques are employed, (2) the catalysts are characterized both after the pretreatments and after the FT synthesis, and (3) the data on steady state Fischer–Tropsch catalyst activity and selectivity after six pretreatment procedures are obtained. The results from this study complement the ones conducted previously in our laboratory with promoted iron catalysts without silica as the binder (15, 18). Results from characterization studies are described in this paper, whereas results from reaction studies are discussed in the accompanying paper (24).

EXPERIMENTAL

Equipment and Procedures

The precipitated iron catalyst used in this study was synthesized by Ruhrchemie AG (Oberhausen–Holten, Germany), and had a nominal composition of 100 Fe/5 Cu/4.2 K/25 SiO_2 (on a mass basis). The preparation procedure was described by Frohning *et al.* (25). The catalyst as received was calcined in air at 300°C for 5 h and then crushed and sieved to granule diameters between 0.25 and 0.50 mm (32 and 60 mesh). The elemental composition was determined by atomic absorption spectrometry (AAS) for iron, copper, and potassium, and gravimetrically for silicon, and was found to be 100 Fe/5.6 Cu/5.1 K/28 SiO_2. The catalyst composition was also determined at Sandia National Laboratories by AAS to be 100 Fe/5 Cu/4 K/27 SiO_2, which is in reasonable agreement with our results and is closer to the nominal catalyst composition.

Catalysts were pretreated in a SS-316 fixed bed reactor (1.25 cm OD, 12 cm long). This unit was used only for characterization studies following pretreatment in different reducing environments. At the end of pretreatment, the catalyst was purged with helium, and the reactor was removed and transferred to a glove box without exposing the catalyst to an oxidizing atmosphere. Typically 1.5–2.5 g of catalyst was used in pretreatment studies.

Powder XRD patterns of the catalyst samples before pretreatment, after pretreatment, and after FT reaction (used catalysts) were obtained on a Geigerflex (Rigaku, Dmax Series) system using Cu$K\alpha$ radiation (λ = 1.54 Å) starting from $2\theta = 2°$ to 85° at a rate of 4°/min. For determinations of particle size by a line broadening (XRLB) method, the region of interest was scanned at a lower rate of 0.5°/min.

The BET surface areas and the pore size distributions of the catalysts before and after pretreatment were determined by N_2 physisorption at 77 K using a Micromeritics Digisorb 2600 system. The samples were degassed at 150°C for 12 h prior to each measurement.

The Mössbauer measurements were conducted at the University of Kentucky, using a constant acceleration spectrometer of standard design (26, 27). The radioactive source consisted of 50–100 mCi of ^{57}Co in a Pd matrix. The samples were in powdered form and were mounted in Plexiglas compression holders to present a thin aspect to the gamma ray beam. Calibration spectra of metallic iron were obtained simultaneously at the other end of the drive. The spectra were analyzed by least-squares regression of a sum of Lorentzian lines to the experimental data. The hyperfine parameters (the isomer shift, the quadrupole splitting, and the magnetic hyperfine field) were obtained from the estimated line positions.

Isothermal reduction experiments with H_2 and CO at atmospheric pressure were carried out in a fixed bed reactor system similar to that used for FT synthesis (15). The system was equipped with an on-line mass spectrometer (Dycor, M200; Ametek, Inc.) and a gas chromatograph (Carle, AGC Series 400). The effluent gases were monitored continuously by mass spectroscopy at one minute intervals by the use of a computerized data acquisition system.

Temperature-programmed and isothermal reduction studies were performed using both 5% H_2/N_2 and 5% CO/He as reductants. Consumption of the CO or H_2 was monitored by a change in the thermal conductivity of the effluent gas stream. A dry ice/acetone bath was used to remove water formed during hydrogen reductions, and a liquid nitrogen bath was used to remove CO_2 formed during the CO reductions. Catalyst sample weights of 10 to 15 mg and a reductant flow rate of 12 cm^3/min were used in all experiments. A temperature ramp of 20°C/min from room temperature to 900°C was used in all temperature-programmed reduction experiments. In isothermal reductions, a ramp of 20°C/min was used until a temperature of 300°C was reached, the latter temperature then being maintained for 12 h for H_2 reduction.

X-ray photoelectron and ion scattering (ISS) spectroscopies were used to determine the abundance and chemical states of surface and near-surface components of the catalysts after calcination and after subsequent reduction treatments in H_2 or CO. Spectra were acquired using a Perkin-Elmer (PHI) Model 5500 spectrometer, which was equipped with a high-pressure inlet chamber that allowed *in situ* calcination and H_2/CO treatments of heated samples. Magnetically coupled transfer rods were than used to transport the treated samples directly into the spectrometer's UHV analytical chamber, without exposure to the atmosphere. All spectra were obtained using samples prepared in the form of pressed wafers. In a typical XPS data acquisition, a pass energy of 29.35 eV, a step increment of 0.125 eV, and a Mg anode power of 400 W were employed. Binding energies were referenced to the C 1*s* line of adventitious carbon at 284.6 eV. In cases where the binding energy of the latter peak could not be accurately determined due to large amounts of surface carbon resulting from exposure of the sample to CO, binding energies were referenced to the K $2p_{3/2}$ peak at 293.0 eV. ISS spectra were obtained using $^3He^+$ ions at a scattering angle of 134.5° and ~1 kV accelerating potential.

Catalyst Handling and Sample Preparation

After pretreatment procedures, the reactor was sealed in an inert gas atmosphere and then transferred to a glove box. The samples for XRD analyses were loaded into sample holders, which were sealed and then placed directly in the X-ray machine. The BET sample tubes were also loaded in the glove box to prevent exposure of the catalyst to an oxidizing environment.

The used catalysts were removed from the fixed bed reactor under an inert atmosphere at the conclusion of the reaction tests. Catalyst samples removed from the top, bottom, and/or middle portions of the reactor were analyzed separately, after magnetic separation from glass beads (used as a diluent during FT synthesis) in the glove box.

RESULTS AND DISCUSSION

BET Surface Area and Pore Size Distribution

The BET-N_2 surface area and the pore volume of the Ruhrchemie catalyst as received were 295 m^2/g and 0.58 cm^3/g, respectively (Table 1). After calcination at 300°C for 6 h the BET surface area and the pore volume were found to be 290 m^2/g and 0.62 cm^3/g, respectively. The BET surface area and the pore volume did not change significantly after calcination, but it is not known whether the as-received catalyst was subjected to any thermal treatment. In general, the addition of silica to iron FT catalysts is known to improve stability of the porous iron oxide/hydroxide network (22, 28). Silica enters the pores of the original network of the catalyst, thus providing a rigid matrix which helps prevent a complete collapse of the pore structure of the catalyst.

However, after reduction with H_2 at 220°C for 1 h the BET surface area decreased to 179 m^2/g. Decrease in the surface area and pore volume can be attributed to a partial collapse of the porous Fe_2O_3/FeOOH network. Hydrogen reduction at 280°C for 1 and 8 h led to further decreases in surface area to 136 and 160 m^2/g, respectively. The H_2 flow rates were different during these two reductions (Table 1), and the degree of reduction to metallic iron after the 1 h reduction was greater than that after the 8 h reduction (Table 3). The pore volumes also decreased significantly after H_2 reductions (Table 1). Similar results were obtained in the previous studies with the Ruhrchemie catalyst (19, 20). Lox *et al.* (19) reported the following values for the BET surface area and the pore volume: as-received catalyst, 318 m^2/g and 0.54 cm^3/g; hydrogen-reduced catalyst at 220°C for 3 h, 168 m^2/g and 0.51 cm^3/g. The surface area reported by Sault (20) after H_2 reduction at 280°C for 4 h was 169 m^2/g.

The BET surface area decreased from 290 to 118 and 99 m^2/g after pretreatment with CO at 280°C and syngas at 310°C, respectively. The decrease in the BET surface area was higher for the CO- or syngas-reduced catalyst than for the H_2-reduced catalyst. Similar trends were seen when the pore volumes of the H_2- and the syngas-reduced

TABLE 1

BET Results for Pretreated Ruhrchemie Catalyst Samples

Run no.	Pretreatment conditions	Surface area (m^2/g)	Pore volume (cm^3/g)	Pore diameter[a] (Å)
As prepared	None	295	0.58	79
Calcined	Air, 300°C, 5 h	290	0.62	86
FA-2351	H_2, 220°C, 1 h, 3550 cm^3/min	179	0.46	103
FA-2391	H_2, 280°C, 1 h, 3160 cm^3/min	136	0.42	124
FA-1821	H_2, 280°C, 8 h, 125 cm^3/min	160	0.49	122
FA-1801	CO, 280°C, 8 h, 125 cm^3/min	118	0.34	115
FA-2551	H_2/CO = 2,210°C, 6 h, 1200 cm^3/min	99	0.31	125

[a] Pore diameter = (4 × pore volume)/surface area.

catalysts are compared. This may be due to the formation of carbonaceous deposits (formed only in the presence of CO), which causes blocking of the pores of the catalyst and results in a lower surface area than that obtained with the H_2-reduced catalyst. Several studies have reported on the formation of carbonaceous deposits (probably in the form of graphitic carbon) on the catalyst after FTS (29–32). Although the carbonaceous deposits were reported to be present after FTS, it is likely that these deposits may also be formed during CO or syngas pretreatment. Results from isothermal CO reduction studies, described below, indicate that there is a possibility of formation of such deposits on the pretreated catalyst.

The pore size distributions of the catalyst after various pretreatments are shown in Fig. 1. The calcined catalyst exhibited a relatively broad pore size distribution (<15–300 Å; 15 Å is the limit of detection, 10 Å = 1 nm) with maxima at about 20 and 200 Å. The pore size distributions after hydrogen and carbon monoxide pretreatments were similar to that of the calcined catalyst (Figs. 1b–1d). The average pore diameter increased slightly on pretreatment with H_2, CO, or syngas (Table 1). Both Lox *et al.* (19) and Dry (22) reported that the average pore size increases after H_2 reduction and after FT synthesis.

Temperature-Programmed Reduction/Isothermal Reduction

The reduction behavior of the Ruhrchemie catalyst was studied by TPR and isothermal reduction. The H_2 TPR profile of the precalcined Ruhrchemie catalyst, determined at a temperature program rate of 20°C/min, is shown in Fig. 2a. Effluent gases were analyzed by both TCD and on-line mass spectrometry. Also, the TCD was calibrated by measuring the peak area resulting from H_2 TPR profile of a standard CuO sample. This calibration enabled quantitative determination of H_2 consumption during reduction of the Ruhrchemie catalyst and positive identification of the dominant peaks in Figs. 2a and 2b. The sharp peak at 340°C is due to the first step of iron reduction ($Fe_2O_3 \rightarrow Fe_3O_4$) while the smaller peak at approximately 300°C arises from the reduction of copper oxide ($CuO \rightarrow Cu$). The broad peak centered at 650°C is due to the reduction of Fe_3O_4 to metallic iron. Thus, it can be seen that the reduction of Fe_3O_4 to Fe is a more difficult step requiring temperatures greater than 600°C for its occurrence in temperature-programmed mode.

In order to better simulate the reduction conditions followed in FTS, isothermal reduction profiles at 280 and 300°C were obtained. Two types of experiments were performed for this purpose. The first involved monitoring the consumption of reductants H_2 and CO using TCD, while the second involved monitoring the formation of products H_2O and CO_2 using mass spectrometry. The former involved the use of smaller amounts of catalysts (10–15 mg) and lower flow rates (12 cm^3/min), whereas the latter used experimental conditions similar to those employed during pretreatment prior to FT synthesis (SV = 3 Nl/g-cat/h).

The isothermal reduction profile at 300°C of the Ruhrchemie catalyst in H_2 monitored using TCD is shown in Fig. 2b. The sharp peak in the H_2 isothermal reduction profile at ~20 min corresponds to the reduction of Fe_2O_3 to Fe_3O_4 and CuO to Cu. The broad peak extending over the entire 900-min treatment period corresponds to the reduction of Fe_3O_4 to Fe. In previous studies it was found that the level of silica influences reduction of Fe_3O_4 to Fe

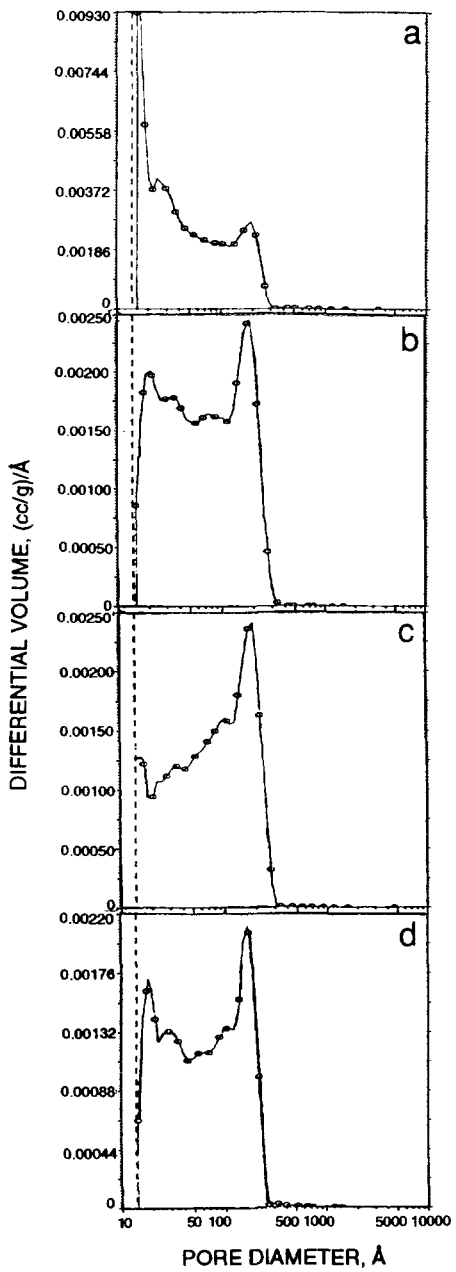

FIG. 1. Pore size distribution of Ruhrchemie catalyst (a) calcined in air at 300°C for 5 h and after pretreatment with (b) H_2 at 220°C for 1 h (flow rate = 3550 cm^3/min), (c) H_2 at 280°C for 1 h (flow rate = 3160 cm^3/min), and (d) CO (125 cm^3/min) at 280°C for 12 h.

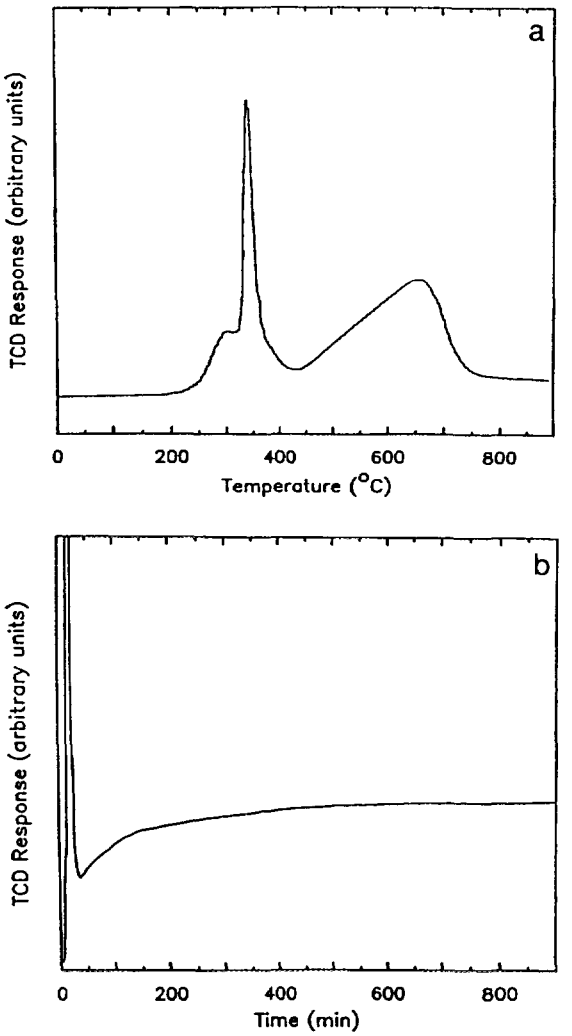

FIG. 2. (a) TPR profile in H_2 at 20°C/min of calcined Ruhrchemie catalyst (16 h in air at 300°C); (b) isothermal reduction profile of calcined Ruhrchemie catalyst at 300°C in H_2.

but does not significantly influence the reductions of Fe_2O_3 to Fe_3O_4 and CuO to Cu (28, 33). The H_2 isothermal reduction profile indicates that even after reduction at 300°C for over 10 h the reduction to metallic iron is incomplete. This is consistent with the XRD and MES results discussed below.

Isothermal reduction profiles were also obtained by switching from He to either H_2 or CO at 280°C for 8 h and monitoring the composition of the effluents by mass spectrometry as a function of time-on-stream. The profiles obtained were similar to that shown in Fig. 2b and are consistent with the two-step reduction process of Fe_2O_3 to metallic iron or iron carbide via magnetite. Initial sharp peaks (corresponding to the reduction of Fe_2O_3 to Fe_3O_4, and of CuO to Cu) were observed after 20 and 30 min of reduction with H_2 and CO, respectively. After this, the reaction proceeds slowly and reaction products H_2O and CO_2 were observed in the effluent gas after 8 h of reduction. In the case of CO reduction, the amount of CO_2 formed during 8 h of reduction was 27.5 mmol/g catalyst. The total amount of CO_2 required for complete reduction of the catalyst is 15.7 mmol/g, whereas the total amount of CO_2 that can be formed assuming complete carbiding of the

TABLE 2

Iron Phases in Pretreated and Used Ruhrchemie Catalyst Samples by X-Ray Diffraction

Run no. Tos (h)	Pretreatment conditions	Pretreated catalyst	Used catalyst after FT synthesis	
FA-0643	H_2, 220°C, 1 h	M(?)	Top:	ε'-C; M
140	3550 cm^3/min		Bottom:	ε'-C; M
FB-0183	H_2, 280°C, 1 h	M; α-Fe	Top:	ε'-C
100	3160 cm^3/min		Bottom:	ε'-C; M
FB-1593	H_2, 280°C, 8 h	M; α-Fe	Top:	ε'-C
154	125 cm^3/min		Bottom:	ε'-C; M
FB-1733	H_2, 280°C, 24 h		Top:	ε'-C
124	125 cm^3/min		Bottom:	ε'-C; M
FB-1588	CO, 280°C, 12 h	χ-C; ε'-C(?)	Average:	M
630	125 cm^3/min			
FB-2290	$H_2/CO = 2$	χ-C	Top:	χ-C
160	310°C, 6 h		Bottom:	M; χ-C
	1200 cm^3/min			

Note. M, Fe_3O_4 (magnetite); spm, superparamagnetic phase; ε'-C, ε'-$Fe_{2.2}C$; χ-C, χ-Fe_5C_2.

catalyst (to $Fe_{2.2}C$) is 3.5 mmol/g. Thus, the total amount of CO_2 formed exceeds the amount of CO_2 that can be accounted for by both reduction as well as carburization of the catalyst. The excess CO_2 is presumably due to the formation of carbonaceous deposits on the catalyst via the Boudouard reaction: $2\ CO \rightarrow CO_2 + C$.

Catalyst Characterization by X-Ray Diffraction and Mössbauer Spectroscopy

The results of XRD and MES analyses of catalyst samples after different pretreatments and after FT synthesis in fixed bed reactors at 250°C, 1.48 MPa (200 psig), 2 Nl/g-cat/h, $H_2/CO = 0.67$ for 100–630 h, are summarized in Tables 2 and 3, respectively. Test duration (time-on-stream, TOS), fixed bed run designations, and pretreatment conditions for each test are listed in the first two columns of these tables. The iron phases in the pretreated and used catalyst samples were assigned by matching the observed lattice spacing values (XRD analysis) or the Mössbauer parameters (hyperfine field and isomer shift values) to those published in the literature. The identification of iron carbide phases in both pretreated and used catalyst samples was rather difficult, since the most intense peaks of all iron carbides are close to each other. However, χ-Fe_5C_2 (Hägg carbide) and ε'-$Fe_{2.2}C$ were identified as the most likely carbides present (Table 2). Three distinct XRD patterns, corresponding to iron carbides with the same stoichiometric formula, Fe_5C_2, and all belonging to a monoclinic crystallographic sructure, have been published in the literature (34–36). Our patterns contain strong lines which belong to all three patterns, but the best match is obtained with the pattern published by Senateur (35). Designation ε'-$Fe_{2.2}C$ refers to the XRD pattern of Barton and Gale (37), which corresponds to pseudo-hexagonal iron carbide with iron atoms in approximately hexagonal close-packed array, which the carbon atoms occupy octahedral interstices. This carbide has been also referred to as ε-Fe_2C carbide. The phases which could not be positively identified due to inadequate matching with strong lines in published patterns and/or overlap with the major lines of other phases present in the sample, are denoted with a question mark (Table 2). The identification of iron phases by Mössbauer spectroscopy was made utilizing published values for Mössbauer parameters from the following references: metallic iron, α-Fe (6, 38, 39); superparamagnetic oxides (5, 6); magnetite, Fe_3O_4 (39, 40); ε'-$Fe_{2.2}C$ carbide (7, 38); and χ-Fe_5C_2 carbide (7, 39, 41).

Pretreated catalyst samples. The as-prepared and calcined catalysts exhibited broad signals indicating that the catalyst was nearly amorphous in nature. Seven poorly defined diffraction peaks coincide with the most intense lines of α-Fe_2O_3 (hematite). The Mössbauer spectra of calcined catalyst were typical for Fe^{3+} in an octahedral oxygen or oxyhydroxide environments (5, 6, 19). Kündig *et al.* (42) have shown that the critical particle diameter for superparamagnetic relaxation in α-Fe_2O_3 at room temperature is 13.5 nm. This is consistent with XRD results which indicate low crystallinity of the calcined sample.

Pretreated catalyst samples after hydrogen reductions. The iron phases after the hydrogen reductions, as determined by XRD, were either magnetite only (reduction at 220°C) or magnetite and metallic iron (reductions

TABLE 3

Iron Phases in Pretreated and Used Ruhrchemie Catalyst Samples by Mössbauer Spectroscopy

Run no. TOS (h)	Pretreatment conditions	Pretreated catalyst (% Fe)	Used catalyst after FT synthesis (% Fe)	
FA-0643 140	H_2, 220°C, 1 h 3550 cm^3/min	100 (spm)	Top: Bottom:	80 (spm); 20 (ε'-C) 59 (spm); 32 (ε'-C); 9 (M)
FB-0183 100	H_2, 280°C, 1 h 3160 cm^3/min	87 (spm), 13 (α-Fe)	Top: Bottom:	57 (spm); 43 (ε'-C) 59 (spm); 41 (ε'-C)
FB-1593 154	H_2, 280°C, 8 h 125 cm^3/min	92 (spm), 8 (α-Fe)	Top: Bottom:	61 (spm); 39 (ε'-C) 69 (spm); 31 (ε'-C)
FB-1733 124	H_2, 280°C, 24 h 125 cm^3/min		Top: Bottom:	48 (spm); 52 (ε'-C) 60 (spm); 40 (ε'-C)
FB-1588 630	CO, 280°C, 12 h 125 cm^3/min	46 (spm), 54 (χ-C)	Average:	27 (spm); 68 (M); 5 (C)
FB-2290 160	H_2/CO = 2 310°C, 6 h 1200 cm^3/min	46 (spm); 54 (χ-C)	Top: Bottom:	63 (spm); 37 (χ-C) 45 (spm); 38 (M); 17 (χ-C)

Note. *M*, Fe_3O_4 (magnetite); spm, superparamagnetic phase; ε'-$Fe_{2.2}C$; χ-C, χ-Fe_5C_2; C, carbide.

at 280°C). The XRD pattern, after reduction with H_2 at 220°C for 1 h, had weak signals at 2θ = 35.4° and 62.7°, which correspond to magnetite. The particle size estimated by X-ray line broadening technique was 50 Å. Lox *et al.* (19) reported that the XRD patterns of the Ruhrchemie catalyst before and after reduction with H_2 at 220°C for 3 h were qualitatively similar and exhibited poorly defined diffraction peaks, which may be attributed to α-Fe_2O_3 and poorly crystalline iron oxide or oxyhydroxide.

The particle sizes of α-Fe, estimated by XRLB method, in samples reduced at 280°C for 1 and 8 h were 80 and 100 Å, respectively. The increase in the particle size with increase in reduction temperature (220 vs 280°C) can be attributed to a partial collapse of the iron pore structure on reduction, resulting in decrease of the specific surface area. The water formed during the reduction with hydrogen is believed to enhance sintering of iron particles (14, 22).

The iron phases after the hydrogen reductions, as determined by MES, were either superparamagnetic oxide (reduction at 220°C) or superparamagnetic oxide and metallic iron (reductions at 280°C). As stated above, in addition to α-Fe, magnetite was also found in samples reduced at 280°C by XRD analysis. It is well known that the reduction of iron oxide (Fe^{3+}) to metallic iron proceeds in two steps via magnetite and that the reduction from magnetite to iron is the slow step in the sequence (15, 28, 43–45). Also, the experimental data illustrating this behavior were presented in the section on isothermal reduction. It is unlikely that the catalyst contained metallic iron but no Fe^{2+}, and it is expected that a portion of superparamagnetic oxide phase is in the form of Fe^{2+}. Lox *et al.* (19) reported that a considerable fraction of iron is in the form of ferrous ions, after H_2 reduction at 220°C for 3 h. Their spectra are qualitatively similar to the ones obtained in this study, but those authors employed the data fitting procedure which resulted in the following assignments: superparamagnetic α-Fe, 20%; ferrous (Fe^{2+}) ions, 76%; and bulk α-Fe_2O_3, 4%.

The fraction of metallic iron after hydrogen reductions at 280°C is very small (8–13%). It is interesting to note that the degree of iron reduction was lower for the catalyst which was exposed to hydrogen for 8 h (8%) than for the one which was reduced for 1 h (13%). However, hydrogen flow rate during the former (8-h duration) was significantly lower than that during the 1-h reduction (Table 3). It has been suggested that the water formed during reduction plays an important role in the determination of the iron phases formed (14, 22). The partial pressure of water is expected to be higher at lower gas flow rates, and this may lead to partial reoxidation of the metallic iron.

Pretreated catalyst samples after carbon monoxide and syngas pretreatments. The iron phases found after pretreatments with CO at 280°C for 12 h and synthesis gas (H_2/CO = 2) at 310°C for 6 h were χ-Fe_5C_2 and possibly ε'-$Fe_{2.2}C$ (CO pretreated catalyst, XRD analysis only). The composition of the catalyst after these two pretreatment procedures, as determined by MES (Table 3), was the same: 54% χ-Fe_5C_2 and 46% superparamagnetic oxide/carbide phase.

The degree of reduction to zero valent iron was significantly higher after CO and syngas pretreatments (54%) than after hydrogen reductions (8–13%). This is consistent with previous observations with a variety of iron Fisher–

Tropsch catalysts that CO is a more effective reducing agent than H_2 (15, 45, 46).

Used catalysts after hydrogen reductions. The XRD patterns of used catalysts after FT synthesis showed much better crystallinity than the reduced samples. The iron phases identified in these samples are pseudo-hexagonal ε'-$Fe_{2.2}C$ iron carbide and magnetite (Table 2). The pseudo-hexagonal iron carbide was the only phase found in samples from the top of the reactor (i.e., near the reactor inlet) in three of the four tests in which hydrogen reductions were employed (Runs FB-0183, FB-1593, and FB-1733), whereas samples from the bottom part of the reactor in all four tests contained both ε'-$Fe_{2.2}C$ and Fe_3O_4. Two phases, ε'-$Fe_{2.2}C$ carbide and superparamagnetic oxide or carbide, were found by MES analysis in all hydrogen-reduced samples from the top and bottom parts of the reactor (Table 3). Also, a small amount of magnetite (9% of spectral area) was found in the sample from the bottom of the reactor in the Run FA-0643. This is in general agreement with results from XRD measurements, except that magnetite was identified by XRD analysis in all four tests in samples from the bottom of the reactor, as well as in the sample from the top portion of the reactor in the Run FA-0643. It is possible that some of the superparamagnetic oxide is in the form of ferrous ions. Low-temperature measurements are needed to determine the nature of iron phases in small particles exhibiting superparamagnetic behavior. The presence of Fe_3O_4 in used catalysts has been reported previously (14, 22, 30, 47). It has been suggested that water vapor formed during FTS is responsible for oxidation of metallic iron and/or iron carbides to Fe_3O_4 (14, 22).

The effective H_2/CO ratios are different in different parts of the reactor. Also, due to formation of water and carbon dioxide during the Fischer–Tropsch synthesis reaction, H_2O/H_2 and CO_2/CO ratios are higher in the bottom part (the reactor exit) than in the top part of the reactor. This results in a reducing environment in the top part of the reactor and an oxidizing environment in the bottom part of the reactor (11). Thus the nature of iron phases as well as their relative amounts may vary along the reactor due to the presence of redox gradients, which was observed in several tests (Tables 2 and 3).

Lox *et al.* (19) also reported results from XRD and MES characterization of the used Ruhrchemie catalysts after 200 h of FT synthesis under a variety of process conditions (P = 11–21 bar, T = 553–623 K, H_2/CO = 3–6). Prior to FT synthesis the catalyst was reduced with hydrogen at 220°C for 3 h. The XRD pattern of the used catalyst exhibited peaks attributed to iron oxides different from α-Fe_2O_3 and a mixture of iron carbides (ε'-$Fe_{2.2}C$, χ-Fe_5C_2, and θ-Fe_3C). The Mössbauer spectrum consisted of a mixture of hexagonal close-packed carbides (59%) and superparamagnetic oxide or carbide (41%). These results, in particular those from MES analysis, are similar to the ones obtained in our study even though both the reduction and reaction conditions employed by Lox *et al.* are not directly comparable to the ones used in our study.

In summary, the Ruhrchemie catalyst reduced by hydrogen at 220–280°C for 1–24 h, consists of a mixture of iron oxides (unreduced α-Fe_2O_3 and Fe_3O_4) and metallic iron. The catalyst composition varies with pretreatment conditions, but the degree of reduction to metallic iron is low in all cases. During the FT synthesis at 250°C, 1.48 MPa (200 psig), 2 Nl/g-cat/h, H_2/CO = 0.67 for 100–155 h, the metallic iron and a portion of iron oxides are carburized to pseudo-hexagonal ε'-$Fe_{2.2}C$ carbide. This is consistent with previous studies in which it was found that the carbide phase formed on hydrogen-reduced silica-supported iron catalysts is primarily ε'-$Fe_{2.2}C$ carbide (2, 7, 48). The bulk composition of the used catalyst was not a strong function of the reduction conditions and consisted of 30–50% ε'-carbide and 50–70% iron oxides or carbides in the form of small particles. Variations in the bulk iron phases in samples taken near the reactor inlet and outlet were not too large, but the crystalline magnetite was found preferentially in samples from the bottom part of the reactor (oxidizing atmosphere).

Used catalysts after carbon monoxide and syngas pretreatments. The iron phases identified by XRD and MES analysis in used catalysts after FT synthesis and pretreatments with CO or syngas were magnetite and χ-carbide. The amount of superparamagnetic oxide/carbide phase varies between 27 and 63% (Table 3). The sample from the bottom part of the reactor in Run FB-2290 contained an appreciable amount of magnetite (38%) in addition to χ-carbide and the superparamagnetic oxide/carbide phases, whereas there was no magnetite in the sample from the top part of the reactor. This is due to the presence of redox gradients in the reactor (oxidizing atmosphere at the reactor outlet).

The sample from Run FB-1588 (CO-pretreated catalyst) was obtained by emptying the reactor and mixing its entire content (i.e., the catalyst and the glass beads). It contains particles from both the top and bottom parts of the reactor and is representative of the average catalyst composition in the reactor. This sample had much more magnetite (68%) than the syngas-pretreated catalyst, which may be related to differences in the duration of the two tests. The CO-pretreated catalyst was on stream for 630 h, whereas the syngas-pretreated catalyst was on stream for 160 h.

After the CO and syngas pretreatments, the α-Fe_2O_3 is partially carburized to monoclinic χ-Fe_5C_2 carbide. During FT synthesis at 250°C some of the χ-carbide is oxidized to magnetite, preferentially near the reactor exit (syngas-pretreated catalyst). The conversion of χ-carbide to magnetite increases with time-on-stream, whereas the fraction of iron in superparamagnetic form decreases with time

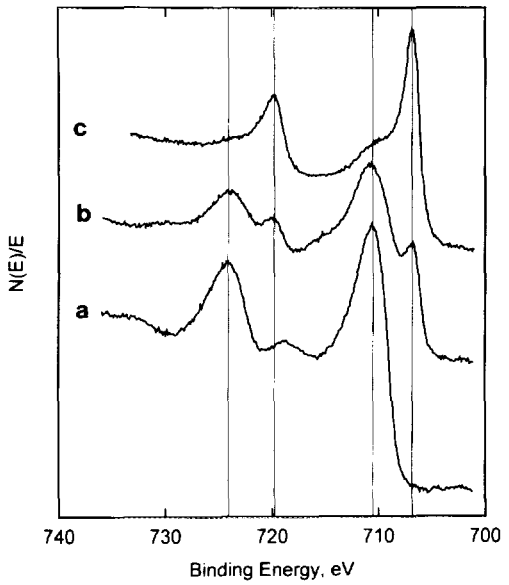

FIG. 3. XPS spectra of Ruhrchemie catalyst in Fe $2p$ region, following (a) calcination for 16 h at 300°C, (b) exposure of (a) to 1 atm of flowing H_2 for 4 h at 300°C, and (c) exposure of (a) to 1 atm of flowing CO for 4 h at 300°C.

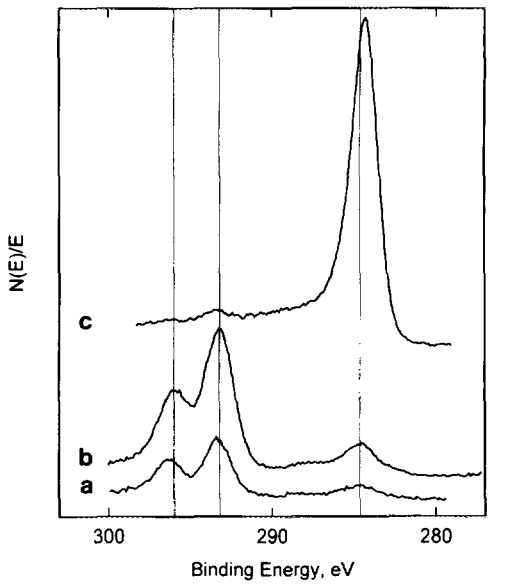

FIG. 4. XPS spectra of Ruhrchemie catalyst in K $2p$ + C $1s$ region, following (a) calcination for 16 h at 300°C, (b) exposure of (a) to 1 atm of flowing H_2 for 4 h at 300°C, and (c) exposure of (a) to 1 atm of flowing CO for 4 h at 300°C.

(CO-pretreated catalyst). It is interesting to note that ε'-carbide does not form during the FT synthesis on the Ruhrchemie catalyst pretreated with either CO or syngas, whereas it was present in used catalyst samples which were initially reduced with hydrogen.

X-Ray Photoelectron Spectroscopy

The programmed and isothermal reduction studies described above reveal overall bulk phase reduction behaviors of the Ruhrchemie catalyst. In order to obtan additional information about the extent of iron reduction and the catalyst composition in the near-surface region, XPS spectra were obtained from samples after initial calcination and after subsequent reduction treatments of calcined samples in H_2 and in CO. Figures 3–5 show XPS spectra in the Fe $2p$, K $2p$ + C $1s$, and O $1s$ regions, respectively, for samples of the Ruhrchemie catalyst after initial calcination in air for 16 h at 300°C (spectra a) and after subsequent *in situ* reduction treatments for 4 h at 300°C in H_2 (spectra b) and in CO (spectra c). Additional data not shown in Figs. 3–5 were also obtained in the Si $2p$, S $2p$, and Cu $2p$ spectral regions of each sample.

The Fe $2p_{3/2}$ peak in Fig. 3a appearing at 710.6 eV, with its accompanying weak $3d \rightarrow 4s$ shake-up satellite peak at 718.7 eV, is due to the Fe^{3+} ions of Fe_2O_3 in the calcined catalyst. These peak positions are in essential agreement with those observed by previous investigators (49), and the spin-orbital splitting of 13.6 eV between the Fe $2p_{3/2}$ and $2p_{1/2}$ peaks further supports this assignment. A small amount of residual adventitious surface carbon remained on the calcined catalyst, as shown by the weak C $1s$ peak appearing at 284.6 eV in Fig. 4a. The peaks that appear at 296.0 and 293.2 eV correspond to the K $2p_{1/2}$ and $2p_{3/2}$ binding energies, respectively, of the potassium promoter.

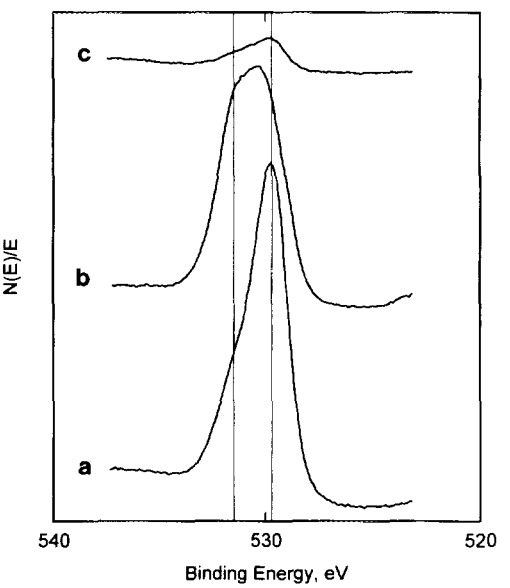

FIG. 5. XPS specra of Ruhrchemie catalyst in O $1s$ region, following (a) calcination for 16 h at 300°C, (b) exposure of (a) to 1 atm of flowing H_2 for 4 h at 300°C, and (c) exposure of (a) to 1 atm of flowing CO for 4 h at 300°C.

The O 1*s* spectrum of the calcined catalyst in Fig. 5a contains a peak at 529.7 eV due to O^{2-} ions in Fe_2O_3, as well as a second peak, appearing as a shoulder at ~531.5 eV, arising from oxygen in the SiO_2 support. The copper promoter in the calcined catalyst existed entirely as Cu^{2+} ions.

In situ treatment of the calcined catalyst in flowing H_2 for 4 h at 300°C resulted in partial reduction of iron in the near-surface region, as shown in Fig. 3b. The narrow Fe $2p_{3/2}$ peak that appears at 706.8 eV is characteristic of reduced metallic Fe^0. The peak that occurred at 710.6 eV in the calcined catalyst has diminished in intensity, has become broadened slightly toward lower binding energies, and may be ascribed to contributions from both Fe^{2+} and Fe^{3+} in Fe_3O_4. The presence of partially reduced Fe^{2+}, following H_2 treatment, is confirmed by the appearance of an additional weak shake-up satellite peak at 715.4 eV. The occurrence of both Fe^0 and Fe_3O_4 in the near-surface region of the H_2-treated catalyst sample is consistent with the corresponding bulk compositions observed by XRD and Mössbauer spectroscopy following similar treatment (Tables 2 and 3). The partial reduction of Fe_2O_3 to Fe_3O_4 is also reflected by the increase of ~0.5 eV in the binding energy of the O 1*s* peak that had occurred at 529.7 eV due to Fe_2O_3 in the calcined catalyst and by a corresponding increase in the relative contribution of the oxygen in SiO_2 (531.5 eV) to the composite O 1*s* peak in Fig. 5b. The copper promoter was completely reduced from Cu^{2+} to metallic Cu^0 by the H_2 treatment. Scans of the S 2*p* spectral region indicated no detectable amounts (i.e., < 0.1%) of near-surface sulfur in either the calcined or H_2-treated samples.

In order to more nearly simulate the temperature conditions used for H_2 reduction pretreatments in the catalytic runs described in the preceding sections, additional experiments were performed in which a catalyst sample was exposed to flowing H_2 at 280°C in the spectrometer's treatment chamber. To monitor the time dependence of the reduction treatment, XPS spectra were obtained at periodic intervals by interrupting the H_2 flow and temporarily transferring the sample *in situ* into the spectrometer's analysis chamber for data acquisition. The results in Fig. 6 show that even 1 h of exposure to H_2 at 280°C (spectrum b) was sufficient to reduce the Fe_2O_3 in the calcined sample to Fe_3O_4, as again indicated by the broadening toward lower binding energies of the original peak due to Fe^{3+} at 710.6 eV and by the appearance of the weak shake-up satellite peak at 715.4 eV. Although the amount of reduced metallic iron, indicated by the narrow peak at 706.8 eV, increases with increasing time of H_2 treatment, most of the formation at Fe^0 had been completed after ca. 4 h. (The slightly larger relative amount of Fe^0 in Fig. 6d compared to that in Fig. 3b may be due to the higher flow rate of H_2 employed in the former experiments, which minimizes possible reoxidation of reduced iron by the H_2O formed during H_2 treatment.) It is also apparent that, even after 16 h of exposure to H_2, a substantial fraction of the iron remains in the form of unreduced Fe_3O_4. Again, no detectable amounts of near-surface sulfur were observed after any of the H_2 treatment times.

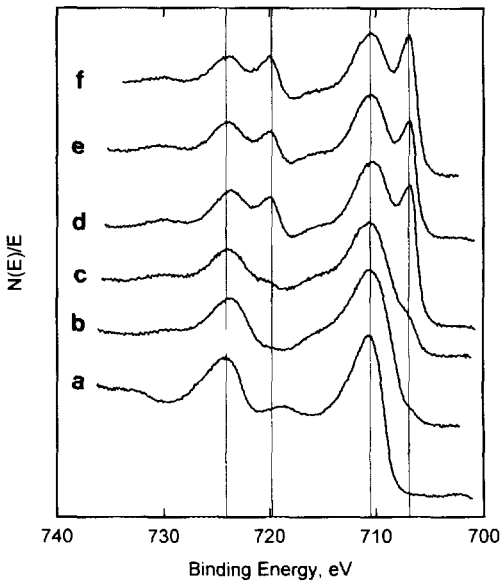

FIG. 6. XPS spectra of Ruhrchemie catalyst in Fe 2*p* region, following (a) calcination for 16 h at 300°C, exposure of (a) to 1 atm of flowing H_2 at 280°C for (b) 1 h, (c) 2 h, (d) 4 h, (e) 8 h, and (f) 16 h.

Treatment of the calcined catalyst in flowing CO for 4 h at 300°C caused much more extensive iron reduction than did the corresponding treatment in H_2. As shown in Fig. 3c, a much smaller amount of unreduced iron remained following exposure to CO than that observed in Fig. 3b. The exact chemical state of the surface iron in the CO-treated catalyst cannot be unambiguously determined from Fig. 3c, however, since the binding energies of metallic Fe^0 and of the Fe in the various iron carbide phases are very similar (49). Indeed, Fig. 4c reveals that a large amount of surface carbon, either graphitic or carbidic, resulted from the CO treatment. The slightly lower binding energy of the C 1*s* peak in Fig. 4c compared to that due to adventitious carbon in Figs. 4a and 4b suggests that a different form of carbon, either graphitic or carbidic, resulted from the CO treatment. It is also apparent from the virtual absence of the K 2*p* peaks in Fig. 4c that, whatever the chemical identity of the carbonaceous species deposited as a result of CO treatment, it almost completely covers the potassium promoter that had been present in the near-surface region of the calcined (and H_2-treated) catalyst. Similarly, the intensities of both components (SiO_2 and FeO_x) of the O 1*s* peak decreased markedly following CO treatment, as is shown in Fig. 5c, and the accompanying Si 2*p* peak at 103.3 eV (not shown in Figs. 3–5) also de-

creased to <5% of its original intensity. This significant attenuation of XPS peaks due to SiO_2 further supports the conclusion that the original catalyst surface became covered by a carbonaceous deposit, since, unlike FeO_x, SiO_2 is unlikely to be chemically affected by the CO treatment. Hence, although the additional presence of metallic Fe^0 cannot be ruled out, it is reasonable to assume that the near-surface region of the CO-treated catalyst consisted largely of the χ-Fe_5C_2 and possibly some ε'-$Fe_{2.2}C$ bulk carbide phases that were observed by XRD and MES (Tables 2 and 3).

Sault (20) and Sault and Datye (21) have previously investigated the reduction behavior of this same Ruhrchemie catalyst in both H_2 and CO, using AES and obtained results in seeming disagreement with those observed in the present study. The AES spectrum of a previously calcined (3 h at 300°C) catalyst sample treated in CO for 12 h at 280°C showed no evidence for deposition of a surface carbon species and was, in fact, virtually identical to the spectrum of a similarly calcined sample treated in H_2 for 1 h at 220°C. Based on the Fe (MVV) region of the spectrum, the authors also concluded that all of the near-surface iron remained in an oxidized form, most likely as a mixture of Fe_xO and Fe_3O_4, following CO treatment. For an identically treated related catalyst that contained no SiO_2 and substantially less potassium promoter (100 Fe/3 Cu/0.2 K), however, the AES spectrum indicated that presence of a substantial amount of surface carbon in a graphitic, not carbidic, form. Based on these results, Sault postulated that the presence of SiO_2 and high levels of potassium promoter effectively prevent reduction of iron to the metallic state during CO activation, thus precluding CO dissociation and carbon deposition on the catalyst surface.

These apparent discrepancies of Sault's results with those of the present study may be due to differences in activation conditions used in the two studies. The catalyst in the present investigation was characterized after the use of somewhat more severe pretreatment conditions (higher temperature) than those used in Sault's AES study. This could account for the greater extent of iron reduction observed by XPS, as well as for the presence of a surface carbon species, following CO treatment. However, the differing surface sensitivities of the AES and XPS techniques may also contribute to the apparent disagreement in results obtained by the two methods. Neglecting work function effects, the kinetic energy of the C (KLL) electrons detected by AES is ~270 eV, corresponding to an escape depth of 7 to 8 Å (~3 lattice layers), while the C 1*s* electrons detected by XPS using a Mg$K\alpha$ X-ray source have a kinetic energy of ~970 eV, resulting in an escape depth of ~15 Å (6 lattice layers) (50). Hence, if the carbon species generated by CO treatment were located primarily in a subsurface bulk phase, it may be detectable by XPS but be unobservable by AES. Such behavior would be consisent with the bulk carbide phases observed by XRD and MES for CO-treated catalysts in the present study.

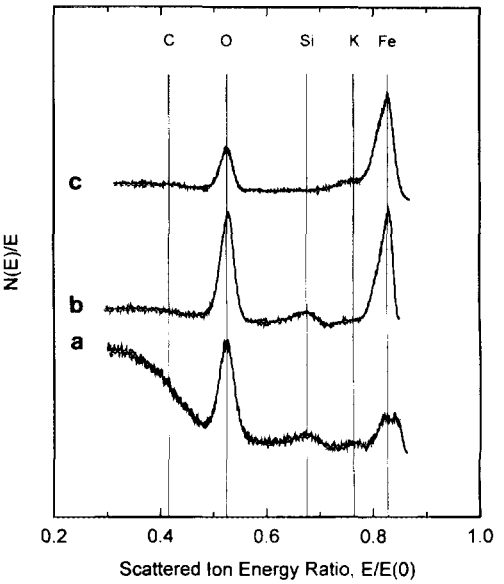

FIG. 7. ISS spectra of Ruhrchemie catalyst following calcination for 16 h at 300°C: (c) initial data collection; (b) after 40 min of exposure to 1 keV $^3He^+$ ion beam; and (c) exposure of (b) to 1 atm of flowing CO for 4 h at 280°C, initial data collection.

In order to obtain additional information about the possible location of the CO-generated carbon species, ion scattering spectroscopy was employed. At sufficiently short data collection times (to avoid surface sputtering effects), the ISS technique detects atoms in only the uppermost surface layer of a solid. The resulting spectra are largely unaffected by subsurface species. ISS spectra were obtained for both the freshly calcined catalyst and for a CO-treated sample and are presented in Fig. 7. For the calcined catalyst (spectrum a), a small amount of residual surface-layer adventitious carbon was observed initially, in agreement with the XPS data in Fig. 4a, but it was gradually sputtered away with increasing time of exposure to the $^3He^+$ ion beam (Fig. 7b). However, following exposure of the sample to flowing CO for 4 h at 300°C and subsequent evacuation, the resulting ISS spectrum (Fig. 7c) showed virtually *no evidence* for a surface-layer carbonaceous species. Furthermore, the O/Fe ratio on the surface decreased by ~50%, while the peak due to surface-layer Si almost completely disappeared. These results are consistent with the existence of a silica supported/promoted carbon-containing, possibly iron carbide, phase, covered by a thin (no more than two or three atomic layers) coating of FeO_x. The bulk carbon-containing phase would be detectable by XRD (if crystalline), MES, and (if the FeO_x layer is sufficiently thin) by XPS, but possibly not by AES, while

the FeO_x surface layer would be observable by both AES and XPS.

It should be noted that all of the surface analysis techniques employed in both studies were performed for freshly calcined samples and for H_2- and CO-treated samples. The actual surface condition of the catalyst during the FT synthesis reaction, of course, may, be quite different from that observed prior to reaction. In particular, after sufficiently long reaction times, the catalyst surface may eventually reach the same condition, regardless of pretreatment. Thus, initial differences between the surface or near-surface compositions of H_2- and CO-pretreated catalysts may not necessarily correlate with steady state catalytic activity/selectivity behavior.

SUMMARY

The as-received Ruhrchemie catalyst had a BET surface area of 295 m^2/g and a pore volume of 0.58 cm^3/g, both of which remained unchanged (within experimental error) after calcination in air at 300°C for 5 h. After different pretreatments with H_2, CO, or syngas, both the BET surface area and the pore volume of the catalyst decreased to 100–180 m^2/g and 0.31 to 0.49 cm^3/g, respectively. The decrease in the surface area and the pore volume is attributed to a partial collapse of the porous iron oxide/hydroxide network, which is stabilized by the presence of silica. In the absence of silica, the surface areas of pretreated precipitated iron catalysts are between 10 and 40 m^2/g (14, 18, 22, 33, 51, 52).

The extent of bulk iron reduction following H_2 and CO pretreatments was studied by isothermal and temperature-programmed reduction. The isothermal and temperature-programmed reduction profiles indicate that the reduction occurs in two steps: facile reduction of Fe_2O_3 to Fe_3O_4, followed by slow reduction of Fe_3O_4 to either metallic iron (H_2 reduction) or an iron carbide (CO pretreatment). The first step is completed in about 15–30 min, whereas the second step is not complete even after 8–10 h at 280–300°C. The amount of CO_2 released during the CO pretreatment at 280°C was greater than the stoichiometric amount needed for complete oxygen removal and complete carburization of iron in the catalyst. It is assumed that this is due to formation of carbonaceous deposits by the Boudouard reaction. The presence of carbonaceous deposits on the catalyst surface was also detected by XPS measurements.

The catalyst composition in the near-surface region, where adsorption and catalysis occur, was studied by X-ray photoelectron spectroscopy, following reduction treatments with H_2 and CO. These results indicate that CO is far more effective in reducing surface iron at 300°C than is H_2. However, even following reduction treatment with CO, a fraction of the surface iron remained in the form of unreduced Fe^{2+}/Fe^{3+} species. The exact chemical nature of the surface iron species after CO treatment could not be unambiguously identified, however, because of the similarity in Fe 2*p* binding energies of metallic iron and of Fe in surface carbide phases. ISS spectra indicate that the carbon deposited as a result of CO treatment exists as a subsurface, possibly carbidic, phase, covered by a thin layer (<10 Å) of FeO_x.

After the reductions with H_2 the α-Fe_2O_3 was partially reduced to either Fe_3O_4 (magnetite) (reduction at 220°C) or to a mixture of Fe_3O_4 and α-Fe (reduction at 280°C). During FT synthesis the α-Fe and a fraction of iron oxides were carburized to pseudo-hexagonal ε'-$Fe_{2.2}C$. The used catalyst samples from the bottom part of the reactor also contained magnetite. After the CO and syngas pretreatments, the α-Fe_2O_3 was partially carburized to χ-carbide. During FT synthesis the χ-carbide was partially converted to Fe_3O_4. With the syngas-pretreated catalyst the χ-carbide content was higher in the sample from the top part of the reactor (reducing atmosphere), while Fe_3O_4 was found in the sample from the bottom part (oxidizing atmosphere). The degree of reduction to zero valent iron was significantly higher after the CO and syngas pretreatments (54%) than after the hydrogen reductions (8–13%).

The effects of pretreatment conditions on the catalyst activity, stability with time, and product distribution are reported in the accompanying paper (24). Results from characterization studies are used to some extent to help explain the observed activity and selectivity trends during FT synthesis with the CO-rich synthesis gas at reaction conditions representative of industrial practice.

ACKNOWLEDGMENTS

This work was supported in part by the U.S. Department of Energy, Pittsburgh Energy Technology Center (Contracts DE-AC22-85PC80011, DE-AC22-89PC89868, and DE-AC22-90PC90039). Dr. M. Koranne conducted some of the isothermal reduction studies.

REFERENCES

1. Matsumoto, H., and Bennett, C. O., *J. Catal.* **53,** 331 (1978).
2. Butt, J. B., *Catal. Lett.* **7,** 61 (1990).
3. Dwyer, D. J., and Somorjai, G. A., *J. Catal.* **52,** 291 (1978).
4. Reymond, J. P., Meriadeau, P., and Teichner, S. J., *J. Catal.* **75,** 39 (1982).
5. Amelse, J. A., Butt, J. B., and Schwartz, L. J., *J. Phys. Chem.* **82,** 558 (1978).
6. Raupp, G. B., and Delgass, W. N., *J. Catal.* **58,** 348 (1979).
7. Raupp, G. B., and Delgass, W. N., *J. Catal.* **58,** 361 (1979).
8. Niemantsverdriet, J. W., and van der Kraan, A. M., *J. Catal.* **72,** 385 (1981).
9. Blanchard, F., Reymond, J. P., Pommier, B., and Teichner, S. J., *J. Mol. Catal.* **17,** 171 (1982).
10. Dictor, R., and Bell, A. T., *J. Catal.* **97,** 121 (1986).
11. Soled, S., Iglesia, E., and Fiato, R. A., *Catal. Lett.* **7,** 271 (1990).
12. Kuivila, C. S., Stair, P. C., and Butt, J. B., *J. Catal.* **118,** 299 (1989).
13. Anderson, R. B., *in* "Catalysis" (P. H. Emmett, Ed.), Vol. 4, p. 29. Van Nostrand–Reinhold, New York, 1956.

14. Anderson, R. B., "The Fischer–Tropsch Synthesis." Academic Press, Orlando, FL, 1984.
15. Bukur, D. B., Lang, X., Rossin, J. A., Zimmerman, W. H., Rosynek, M. P., Yeh, E. B., and Li, C. *Ind. Eng. Chem. Res.* **28,** 1130 (1989).
16. Pennline, H. W., Zarochak, M. F., Stencel, J. M., and Diehl, J. R., *Ind. Eng. Chem. Res.* **26,** 595 (1987).
17. Zarochak, M. F., and McDonald, M. A., *in* "Seventh DOE Indirect Liquefaction Contractors' Meeting Proceedings" (G. Cinquegranne and N. Narain, Eds.), p. 96. U.S. Department of Energy, Pittsburgh Energy Technology Center, Pitsburgh, PA, 1987.
18. Bukur, D. B., Koranne, M., Lang X., Rao, K. R. P. M., and Huffman, G. P., *Appl. Catal.*, in press.
19. Lox, E. S., Marin, G. B., De Grave, E., and Bussiere, P., *Appl. Catal.* **40,** 197 (1988).
20. Sault, A. G., *J. Catal.* **140,** 121 (1993).
21. Sault, A. G., and Datye, A. K., *J. Catal.* **140,** 136 (1993).
22. Dry, M. E., *in* "Catalysis—Science and Technology" (J. R. Anderson and M. Boudart, Eds.), Vol. 1, p. 160. Springer-Verlag, New York, 1981.
23. Bukur, D. B., Ledakowicz, S., and Manne, R. K., *in* "Indirect Liquefaction Contractors' Review Meeting Proceedings" (G. J. Stiegel and R. D. Srivastava, Eds.), p. 221. U.S. Department of Energy, Pittsburgh Energy Technology Center, Pittsburgh, PA, 1990.
24. Bukur, D. B., Nowicki, L., Manne, R. K., and Lang, X., *J. Catal.* **155,** 366 (1995).
25. Frohning, C. d., Rottig, W., and Schnur, F., *in* "Chemierohstoffe aus Kohle" (J. Falbe, Ed.), p. 234. Thieme, Stuttgart, 1977.
26. Huffman, G. P., and Huggins, F. E., *Fuel* **47,** 592 (1978).
27. Huffman, G. P., *CHEMTECH* **10,** 504 (1980).
28. Bukur, D. B., Lang, X., Mukesh, D., Zimmerman, W. H., Rosynek, M. P., and Li., C., *Ind. Eng. Chem. Res.* **29,** 1588 (1990).
29. Vogt, E. T. C., van Dillen, A. J., and Geus, J. W., *in* "Catalyst Deactivation" (B. Delmon and G. F. Froment, Eds.), p. 221. Elsevier, Amsterdam, 1987.
30. Davis, B. H., and Tungate, F. L., *in* "Indirect Liquefaction Contractors' Review Meeting Proceedings," (G. J. Stiegel and R. D. Srivastava, Eds.), p. 275. U.S. Department of Energy, Pittsburgh Energy Technology Center, Pittsburgh, PA, 1991.
31. Bonzel, H. P., and Krebs, H. J., *Surf. Sci.* **109,** L527 (1981).
32. Wachs, I. E., Dwyer, D. J., and Iglesia, E., *Appl. Catal.* **12,** 201 (1984).
33. Li, C., "Effect of Potassium and Copper Promoters on Reduction Behavior of Precipitated Iron Catalysts" Ph.D. Dissertation, Texas A & M University, 1988.
34. Hoffer, L. J. E., Cohn, E. M., and Peebles, W. C., *J. Am. Chem. Soc.* **71,** 189 (1949).
35. Senateur, J. P., *Ann. Chim. (Paris)* **2,** 103 (1967).
36. Dirand, M., *Afr. Acta Metall.* **31,** 1089 (1983).
37. Barton, G. H., and Gale, B., *Acta Crystallogr.* **17,** 1460 (1964).
38. Bianchi, D., Borcar, S., Teule-Gay, F., and Bennett, C. O., *J. Catal.* **82,** 442 (1983).
39. Satterfield, C. N., Hanlon, R. T., Tung, S. E., Zou, Z., and Papaefthymiou, G. C., *Ind. Eng. Chem. Prod. Dev.* **25,** 407 (1986).
40. Vogler, G. L. Jiang, X.-Z., Dumesic, J. A., and Madon, R. J., *J. Catal.* **89,** 116 (1984).
41. Matyi, R. J., Butt, J. B., and Schwartz, L. H., *J. Catal.* **91,** 185 (1985).
42. Kündig, W., Bommel, H., Constabaris, G., and Lindquist, R. H., *Phys. Rev.* **142,** 327 (1966).
43. Hofer, L. J. E., *in* "Catalysis" (P. H. Emmett, Ed.), Vol. 4, p. 373. Van Nostrand–Reinhold, New York, 1956.
44. Brown, R., Cooper, M. E., and Whan, D. E., *Appl. Catal.* **3,** 177 (1982).
45. Leith, I. R., and Howden, M. G., *Appl. Catal.* **37,** 752 (1988).
46. Richard, M. A., Soled, S. L., Fiato, R. A., and DeRites, B. A., *Mater. Res. Bull.* **18,** 829 (1983).
47. Berry, F. J., and Smith, M. R., *J. Chem. Soc. Faraday Trans. I* **85,** 467 (1989).
48. Niemantsverdriet, J. W., van der Kraan, A. M., van Dijk, W. L., and van der Baan, H. S., *J. Phys. Chem.* **84,** 3363 (1980).
49. Kuivila, C. S., Butt, J. B., and Stair, P. C., *Appl. Surf. Sci.* **32,** 99 (1988).
50. Somorjai, G. A., "Chemistry in Two Dimensions: Surfaces." Cornell University Press, Ithaca, New York, 1981.
51. Kölbel, H., *in* "Actes de Deuxieme Congres International de Catalyse," Vol. 2, p. 2075. Technip, Paris, 1960.
52. Kölbel, H., and Giehring, H., *Brennst. Chem.* **44,** 343 (1963).